Cell Reports
Article

A pSMAD/CDX2 Complex Is Essential for the Intestinalization of Epithelial Metaplasia

Luigi Mari,[1,2,6] Francesca Milano,[1,2,3,6] Kaushal Parikh,[1,2,6] Danielle Straub,[1,2,6] Vincent Everts,[4] Kees K. Hoeben,[4] Paul Fockens,[2] Navtej S. Buttar,[5] and Kausilia K. Krishnadath[1,2,*]
[1]Centre for Experimental & Molecular Medicine, Meibergdreef 9, 1105AZ Amsterdam, the Netherlands
[2]Department of Gastroenterology & Hepatology, Academic Medical Center, Meibergdreef 9, 1105AZ Amsterdam, the Netherlands
[3]Section of Hematology and Clinical Immunology, Department of Internal and Experimental Medicine, Ospedale S. Maria della Misericordia, University of Perugia, 06156 Perugia, Italy
[4]Core facility Cellular Imaging/LCAM-AMC, Meibergdreef 9, 1105AZ Amsterdam, the Netherlands
[5]Division of Gastroenterology and Hepatology, Mayo Clinic, Rochester, MN 55902, USA
[6]Co-first author
*Correspondence: k.k.krishnadath@amc.uva.nl
http://dx.doi.org/10.1016/j.celrep.2014.03.074

SUMMARY

The molecular mechanisms leading to epithelial metaplasias are poorly understood. Barrett's esophagus is a premalignant metaplastic change of the esophageal epithelium into columnar epithelium, occurring in patients suffering from gastroesophageal reflux disease. Mechanisms behind the development of the intestinal subtype, which is associated with the highest cancer risk, are unclear. In humans, it has been suggested that a nonspecialized columnar metaplasia precedes the development of intestinal metaplasia. Here, we propose that a complex made up of at least two factors needs to be activated simultaneously to drive the expression of intestinal type of genes. Using unique animal models and robust in vitro assays, we show that the nonspecialized columnar metaplasia is a precursor of intestinal metaplasia and that pSMAD/CDX2 interaction is essential for the switch toward an intestinal phenotype.

INTRODUCTION

Barrett's esophagus (BE) is defined as the replacement of normal stratified squamous epithelium with columnar epithelium in the distal part of the esophagus. This metaplastic columnar epithelium can be classified into various types depending on specific histological features. The most common are several nonintestinal and the specialized intestinal type of columnar metaplasia; the latter is also referred to as intestinal metaplasia (IM). IM is associated with a higher risk of developing esophageal adenocarcinoma (EAC) (Chandrasoma et al., 2007). BE develops in 15%–20% of patients suffering from chronic gastroesophageal reflux disease (Spechler et al., 2010). Currently, there are no robust molecular biomarkers to detect disease and predict progression, whereas there is no molecular cure for BE. This would require a much greater understanding of the molecular events involved in the process of metaplasia.

Recently, there has been more focus on the role of transcription factors in the development of metaplasia. These factors include the caudal-related homeobox family members Caudal type Homeobox 1 (CDX1) and Caudal type Homeobox 2 (CDX2) (Huo et al., 2010; Kazumori et al., 2006, 2009), factors such as GATA binding protein 4 (GATA4) (Chen et al., 2008), GATA binding protein 6 (GATA6) (Wang et al., 2009), Hypoxia-inducible factor 1 alpha (HIF-1alpha), Hypoxia-inducible factor 2 alpha (HIF-2alpha) (Griffiths et al., 2007), SRY (sex determining region Y)-box 9 (SOX9) (Wang et al., 2010; Clemons et al., 2012), Kruppel-like factor 4 (KLF4) (Kazumori et al., 2011), and HOX genes (di Pietro et al., 2012). However, in vivo confirmation of their importance is rather limited. Overexpression of CDX2 in the mouse esophagus under the *cytokeratin 14* (*K14*) promoter failed to induce columnar metaplasia (Kong et al., 2011), suggesting that CDX2 alone is insufficient to induce columnar metaplasia, unlike the metaplasia of the stomach, where overexpression of CDX2 under the H^+/K^+*ATPase* promoter clearly leads to intestinal metaplasia of the stomach (Mutoh et al., 2002).

A number of morphogens have also been identified as important contributors to BE pathogenesis. Our group has shown that in vitro stimulation of esophageal cells with Bone Morphogenetic Protein 4 (BMP4) and activation of its downstream target phosphorylated mothers against decapentaplegic 1/5/8 (pSMAD1/5/8; pSMAD) induces the expression of columnar type of genes but does not lead to IM (Milano et al., 2007). Others have shown that overexpression of Sonic Hedgehog (Shh) induces BMP4 in the stroma, which upregulates SOX9 and columnar cytokeratins in the epithelium (Wang et al., 2010). All these studies identify certain factors that are necessary for the development of the columnar epithelium, but none of these individual factors is sufficient for the development of IM suggesting that other mechanisms are involved.

In the current study, we observed that in vivo overexpression of BMP4 induces a columnar phenotype. Similar to the nonintestinal type of columnar metaplasia observed in humans (Nemeth et al., 2012), these glands express pSMAD and several columnar markers; however, they lack expression of IM markers such as CDX2 and Mucin 2 (MUC2) (Mesquita et al., 2003). In a microsurgical murine model, we demonstrate the sequential process of

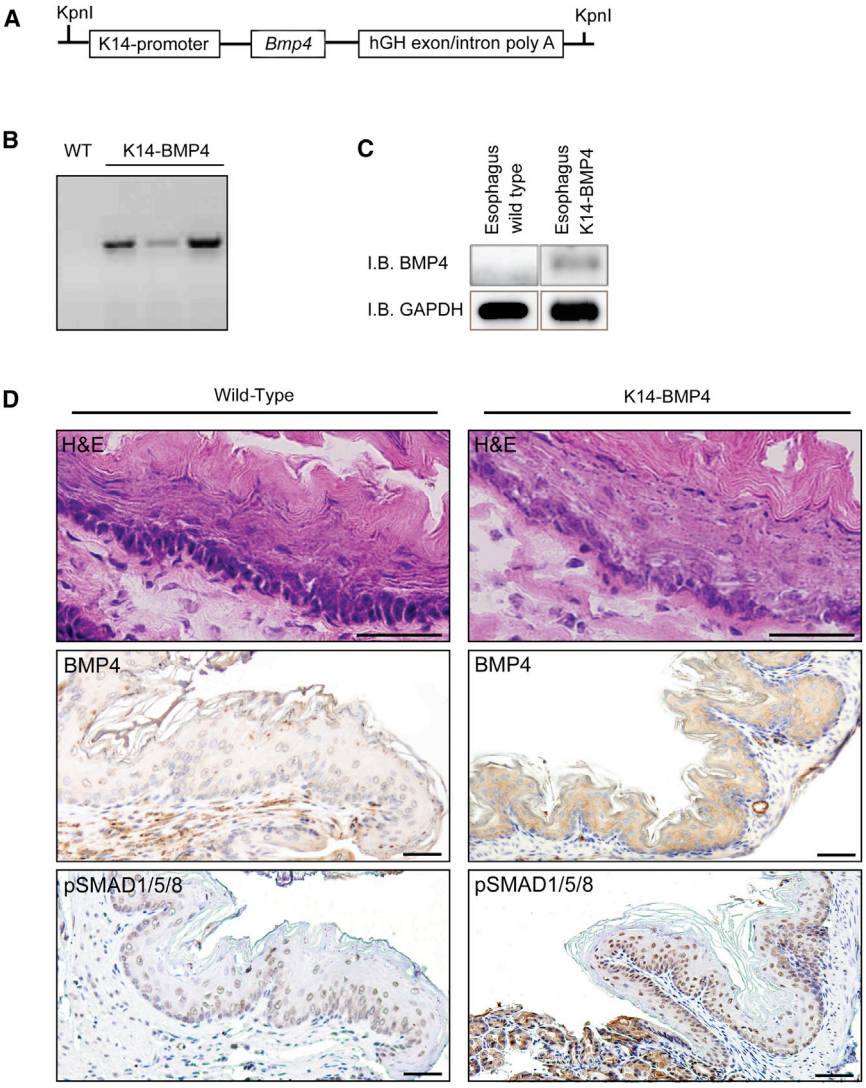

Figure 1. Characterization of K14-BMP4 Mouse

(A) *Bmp4* cDNA was subcloned into the K14-hGH polyA plasmid.

(B) Genotyping PCR for K14-BMP4 fragment.

(C) Western blot expression of BMP4 in the esophagus of wild-type (WT) and K14-BMP4 mice.

(D) Hematoxylin and eosin (H&E), BMP4, and pSMAD staining of WT and K14-BMP4 mice esophagi (scale bar, 200 μm).

See also Figure S1.

nonspecialized columnar metaplasia that develops as a precursory lesion and leads to the development of IM, where coexpression of pSMAD, CDX2, and MUC2 are observed. From in vitro experiments, we found a synergistic collaboration between the two nuclear transcription factors CDX2 and pSMAD, which drives development of an intestinal phenotype in epithelial cells. These findings provide insights in the development of the premalignant IM and reveal key molecular targets for developing novel preventive treatments.

RESULTS

BMP4 Activation Is Required for Columnar Metaplasia at the Squamocolumnar Junction but Is Not Sufficient for Intestinal Metaplasia in a Transgenic Mouse Model

Murine *Bmp4* cDNA was subcloned into the K14-hGH poly (A) plasmid (Figure 1A) and injected into CB6F1 one-cell embryos to generate the K14-BMP4 mice (Guha et al., 2002) (Figure 1B). The esophageal epithelium of the BMP4 mouse compared to the wild-type controls revealed vacuolization of nuclei and a widened zona spinosum, indicating "delayed" keratinization of the cells (Figures 1D, H&E). Immunohistochemistry (IHC) showed increased expression of BMP4 (Figure 1D) in the basal and suprabasal cells and excreted BMP4 in the intercellular space between the nonkeratinizing and keratinizing layers. Nuclear expression of pSMAD, the downstream target of BMP4, was increased in the transgenic animals, whereas only weakly positive in the wild-type (Figure 1D). We also noticed that the K14-BMP4 mice had increased expression of Noggin, a natural inhibitor of BMPs, in the underlying stroma and muscularis mucosa as compared to the wild-type. Noggin expression was highest in the proximal tubular esophagus as compared to the fore-stomach (Figure S1).

In 20-week-old animals, we observed the spontaneous appearance of columnar glandular structures at the squamocolumnar junction (SCJ) in the fore-stomach of the transgenic animals (Figure 2A). IHC on these glandular structures showed positive staining for the squamous markers, cytokeratin 14 (K14), cytokeratin 5 (K5), and p63 (Figures 2Bi, ii, and iii) as well as for the columnar markers pSMAD (Figure 2Biv), cytokeratin 19 (K19) (Figure 2Bv), and cytokeratin 8 (K8) (Figure S2A). These partially multilayered glands are positive for Alcian blue (Figure 2Bvi) and weakly positive for Trefoil Factor 2 (TFF2) (Figure 2Bvii) but are negative for MUC5AC, MUC2, and CDX2 (Figure S2A). These glands are negative for the protein H^+/K^+ATPase pump (Figure S2A), confirming the lack of parietal cells. The basal layer of both the esophagus and the metaplastic glands is positive for K14 and pSMAD (Figure S2B).

To understand the origin of the glands in our model, we performed IHC for cell markers of both the squamous epithelium and columnar/gastric cardia. Figure 2B shows that these glands contain a subset of cells positive for the squamous stem cell marker p63 (Senoo et al., 2007; Yang et al., 1999), and another subset of cells is strongly positive for K19 and weak for TFF2,

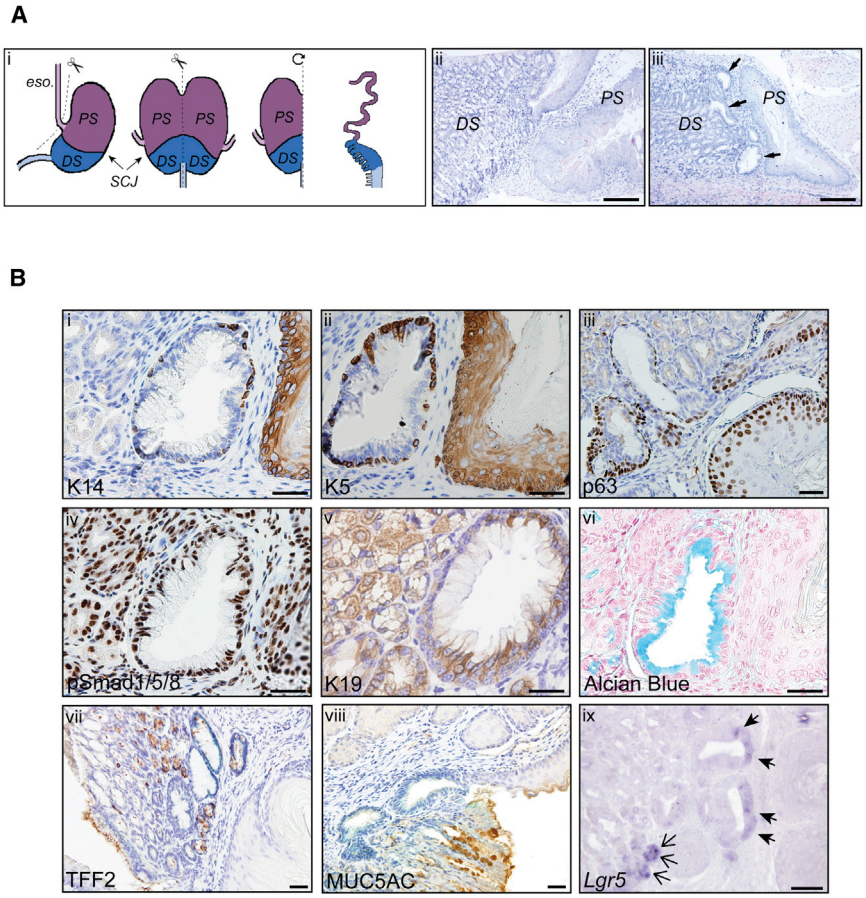

Figure 2. Characterization of Metaplastic Glands at the SCJ in the Fore-stomach of K14-BMP4 Mice

(A) (i) Anatomical overview of the dissected mouse esophagus and stomach, containing the proximal stomach (PS), which is lined with squamous epithelium, the distal stomach (DS), which has columnar glands with parietal cells and the squamocolumnar junction (SCJ). (ii) H&E of the SCJ of WT and (iii) K14-BMP4 mice. Metaplastic columnar glands at the SCJ in the transgenic animals (arrows) (scale bar, 500 μm).

(B) IHC of glands at the SCJ of the K14-BMP4 mouse show cells with expression of squamous markers K14 (i), K5 (ii), and p63 (iii) along with columnar markers K19 (v), pSMAD (iv), Alcian blue (vi), TFF2 (vii), and MUC5AC (viii). RNA ISH for *Lgr5* in the metaplastic glands (closed arrows) along with a normal adjacent cardia gland (open arrows) (ix). Scale bar, 200 μm.

See also Figure S2.

which are markers shown to label gastric progenitor cells (Means et al., 2008; Quante et al., 2010). RNA in situ hybridization for the intestinal stem cell marker *Lgr5* (Barker et al., 2007), known to be expressed in BE (Becker et al., 2010), was positive for a subset of cells in these glands (Figure 2Bix).

In conclusion, the glands seen in this transgenic model include a mixture of cell lineages and resemble the nonspecialized columnar epithelium (NSCE) observed in humans (Glickman et al., 2001a; Chaves et al., 2002; Srivastava et al., 2007). Earlier studies in humans have suggested that a transitional multilayered epithelium and NSCE may indicate stages between squamous and intestinal metaplasia (Chandrasoma, 1997). Our findings suggest that BMP4 is important in the initiation of the metaplastic process that leads to NSCE at the SCJ in the forestomach of BMP4-overexpressing mice but is insufficient for an intestinal phenotype.

pSMAD, CDX2, and MUC2 Are Expressed in Intestinal Metaplasia, which Appears Only at a Later Stage in a Surgical Reflux Mouse Model

Because BMP4 is insufficient to induce IM, we aimed to identify the different stages at which important markers for IM including CDX2 and MUC2 (Steininger et al., 2005) appear by using a microsurgical mouse model. In this model, reflux and subsequently metaplasia of the esophageal mucosa is induced via an esophageal-jejunostomy following a novel method (N.S. Buttar and C.J. DeMars, 2011, Digestive Disease Week, abstract).

At week 12, this mouse model develops a transitional zone at the anastomosis site, the neosquamocolumnar junction (neoSCJ), with metaplastic columnar epithelium appearing distally of the neoSCJ and in between the inflamed squamous epithelium (Figure 3A). The columnar epithelium in this zone resembles the nonspecialized columnar type of epithelia as seen in BE patients (Figure S3B) and as described earlier (Srivastava et al., 2007). At week 12 (Figure 3B), the inflamed squamous and the metaplastic columnar epithelia express high levels of pSMAD. Only a few columnar cells exhibit nuclear CDX2 expression, whereas the expression of MUC2 is virtually absent. At week 16, the metaplastic columnar zone has expanded and exhibits more glands and villi with histological features that increasingly resemble the human type of IM (Figures S3B) (Srivastava et al., 2007). Besides the high nuclear expression of pSMAD, the intestinal metaplasia also shows high CDX2 expression along with the expression of MUC2 (Figure 3B). Additionally, PAS staining is positive, suggesting the presence of mucin producing cells (Figure S3A).

These observations indicate that in the surgical model the development of IM requires a stepwise series of events in which a nonintestinal type of metaplasia resembling the human NSCE precedes the development of IM.

Glands in the Surgical Metaplasia Model Do Not Arise from Lgr5^{+} Progenitor Cells

Because Lgr5-expressing cells have been observed in human BE, it has been suggested that the stem cells that give rise to BE may originate from the neighboring columnar epithelia

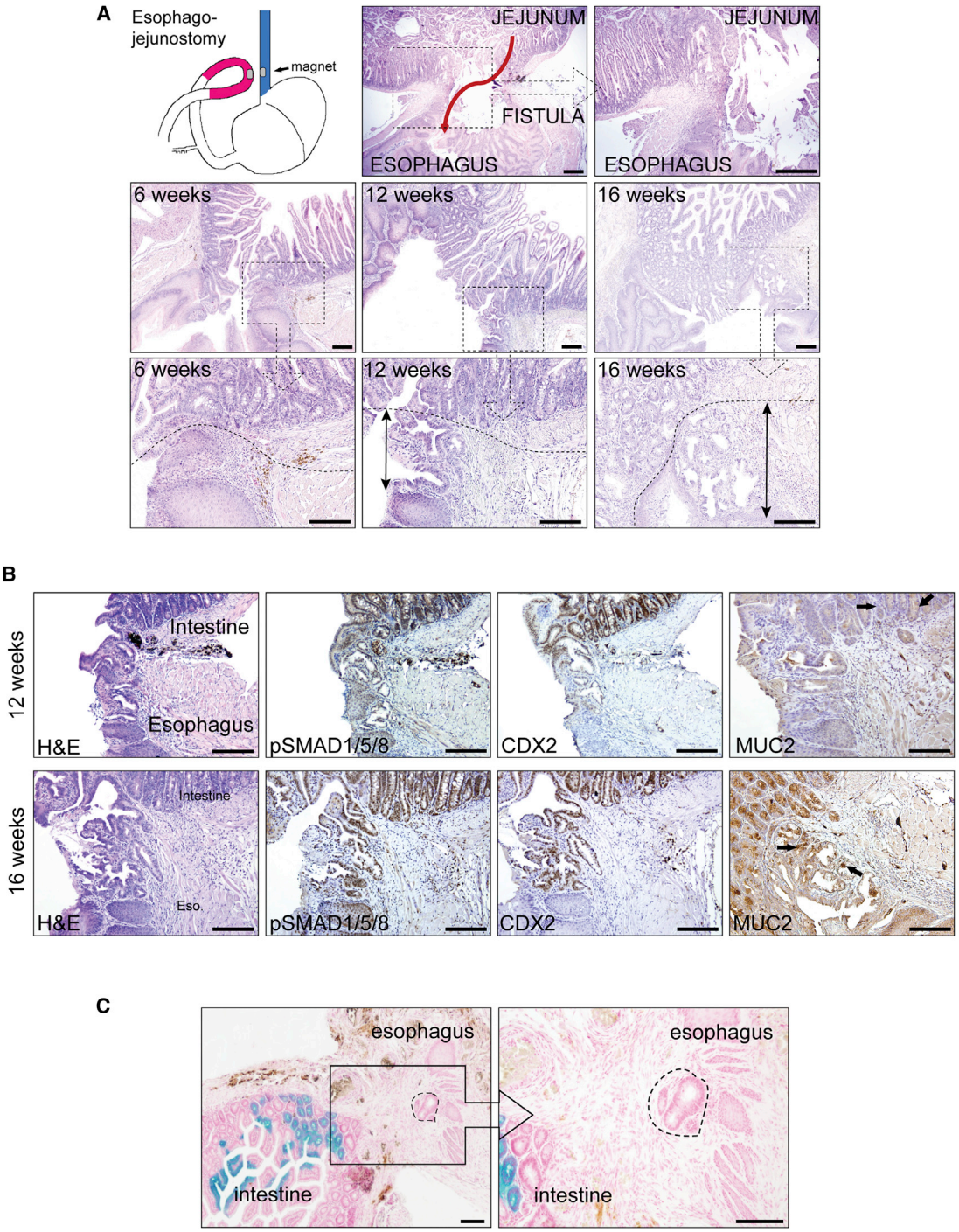

Figure 3. Expression of Epithelial Markers and Lineage Tracing Results during Metaplasia Development in the Esophagus in a Surgical Mouse Model

(A) Mouse model following Buttar's esophagojejunostomy shows the positioning of two magnets. After 6 weeks, an esophageal-jejunal fistula is formed allowing reflux of bile into the esophagus (red line). Right upper panel shows higher magnification of middle upper panel. H&E staining representative of the neo-SCJ at 6, 12, and 16 weeks postsurgery. The dotted black line indicates the anastomosis, and the double-headed arrows indicate the metaplastic area. Scale bar, 500 μm.

(B) H&E and IHC of inflamed squamous and metaplastic region for pSMAD, CDX2, and MUC2 at 12 and 16 weeks after surgery. Arrows indicate MUC2-positive cells. Scale bar, 500 μm.

(C) Representative images of β-gal staining in Lgr5-cre-Rosa26-lacZ mice. The black dotted line indicates the metaplastic glands at the anastomosis site in the esophagus 12 weeks after surgery. Scale bar, 500 μm.

See also Figures S2 and S3.

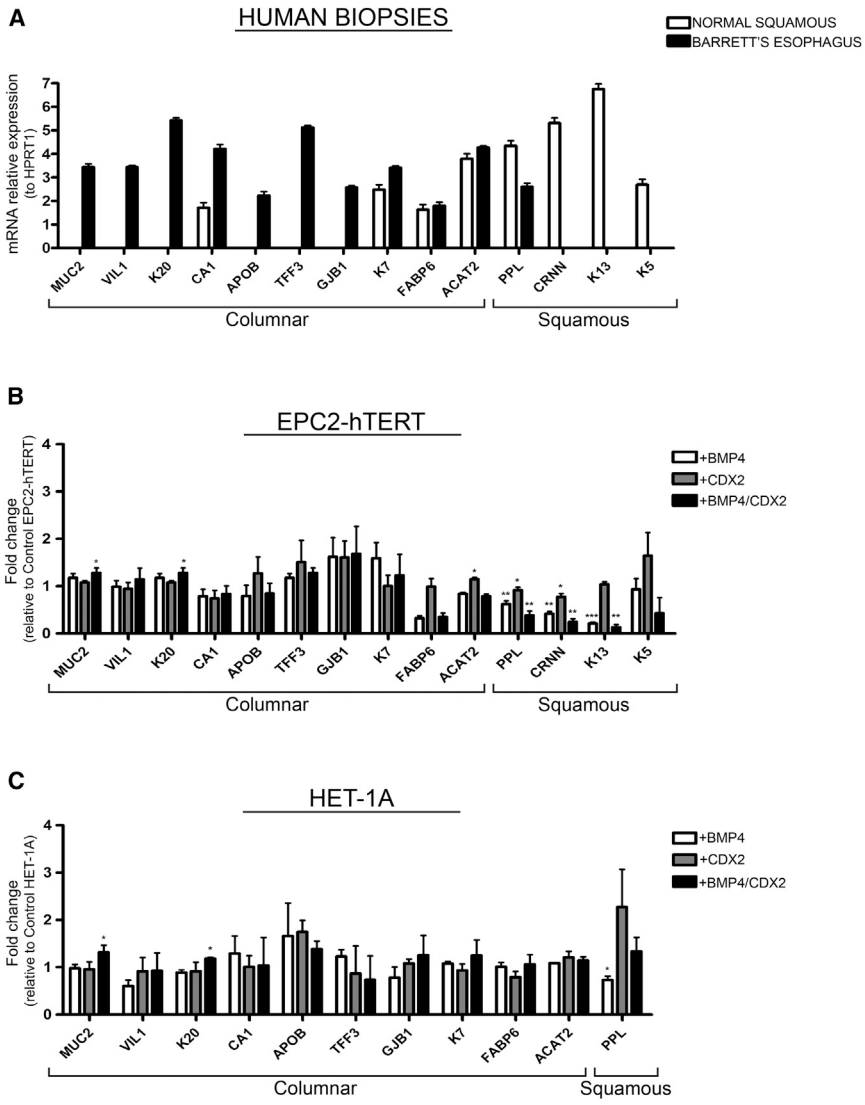

Figure 4. qPCR Indicates that BMP4 Regulates Expression of Epithelial Markers, whereas BMP4 and CDX2 Induce MUC2 Expression

(A) Expression of columnar and squamous specific genes in squamous and BE patient biopsies by real-time qPCR arrays. Data are representative of two independent experiments with two technical replicates and were normalized to the expression level of *HPRT1*.

(B and C) Expression of the same set of genes in EPC2-hTERT and HET-1A cells under four conditions: Control (unstimulated/untransfected), transfected with CDX2, stimulated with BMP4 (100 ng/ml for 48 hr), transfected with CDX2, and stimulated with BMP4. Results are expressed relative to the baseline expression levels of the control cells EPC2-hTERT or HET-1A (Figure S4). Error bars indicate the SEM of the mean. Paired t test *$p < 0.05$, **$p < 0.01$, ***$p < 0.001$, $n = 4$. See also Figure S4.

harboring Lgr5$^+$ stem cells (Quante et al., 2012; Becker et al., 2010; von Rahden et al., 2011). To investigate if the metaplasia observed in the esophagus in our surgical model originates from Lgr5$^+$ progenitor cells, we performed lineage tracing by creating the esophagojejunostomy in Lgr5-EGFP-ires-CreERT2/Rosa26-lacZ mice (n = 15) (Barker et al., 2007). The anastomosis was performed 1 week after administering Tamoxifen, and metaplasia was allowed to develop over 6 (n = 5), 12 (n = 5), and 16 weeks (n = 5). In this model, the progeny of Lgr5$^+$ stem cells will retain and express the lacZ gene, which after exposure to β-galactosidase (β-gal) will turn blue. None of the glands in all the animals studied showed positive β-gal staining, although the normal jejunum lying adjacent to the site of the metaplasia showed entire blue crypts and villi indicating successful lineage tracing in the jejunum (Figure 3C). Our data suggest that Lgr5$^+$ progenitors are not at the basis of the columnar metaplasia that develops in the tubular esophagus and at the neo-SCJ in our surgical model.

BMP4 Stimulation of CDX2-Transfected Cells Induces the Expression of Intestinal Type of Genes

Based on previous gene profiling studies, we selected a panel of squamous genes: Periplakin (*PPL*), cornulin (*CRNN*), cytokeratin 13 (*K13*), cytokeratin 5 (*K5*), and columnar genes: Villin 1 (*VIL1*), carbonic anhydrase I (*CA1*), apolipoprotein B (*APOB*), *TFF3*, gap junction protein beta 1 (*GJB1*), cytokeratin 7 (*K7*), fatty acid binding protein 6 (*FABP6*), acetyl-CoA acetyltransferase 2 (*ACAT2*), and putative CDX2 target genes: *MUC2* and cytokeratin 20 (*K20*) that are known to be expressed in BE (Milano et al., 2007; van Baal et al., 2013; Liu et al., 2007). We analyzed their basal gene expression levels in esophageal biopsies from patients with and without BE, and in the human squamous esophageal epithelial cell lines HET-1A and EPC2-hTERT using custom-made quantitative PCR (qPCR) arrays. We studied both cell lines before and after CDX2 transfection, and with and without BMP4 stimulation. The qPCR results confirmed higher expression levels of the columnar genes in the BE samples as compared to the squamous biopsies, except for *K7*, *FABP6*, and *ACAT2*. As expected, the expression of squamous genes was higher in the squamous biopsies (Figure 4A).

Expression levels of these genes showed similar patterns between the squamous biopsies and the EPC2-hTERT cell line. HET-1A cells lacked the expression of several squamous markers such as *CRNN*, *K13*, and *K5* (Figure S4B), confirming that this cell line has an incomplete squamous phenotype (Underwood et al., 2010). BMP4 stimulation of CDX2-transfected and -nontransfected cells significantly downregulated the

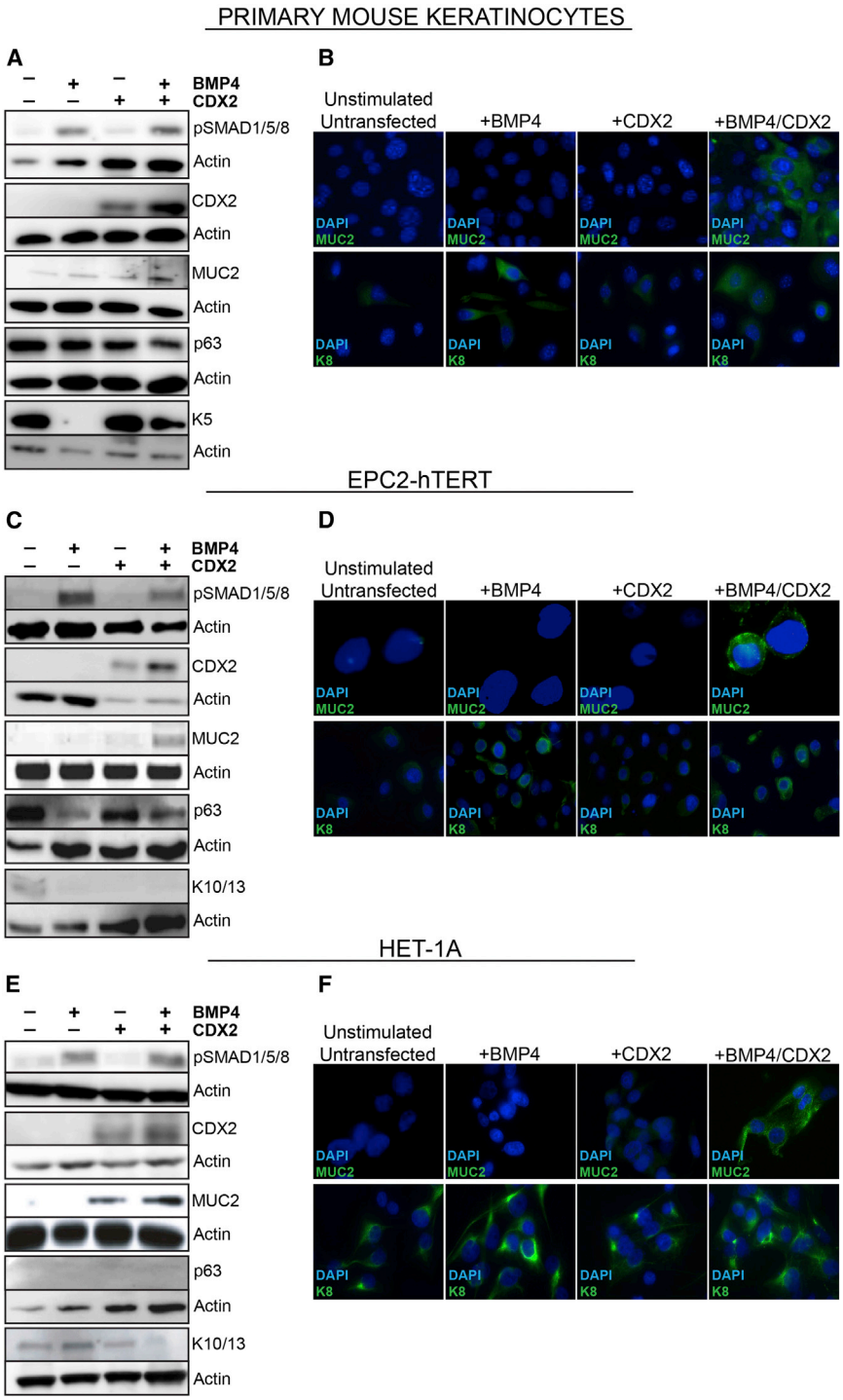

Figure 5. BMP4 Modulates Squamous Markers, whereas BMP4 and CDX2 Together Drive the Expression of MUC2

(A, C, and E) Western blot of primary keratinocytes, EPC2-hTERT, and HET-1A cells for pSMAD, CDX2, MUC2, p63, K5, and K10/13 under four conditions: control (unstimulated/untransfected) transfected with CDX2, stimulated with BMP4 (100 ng/ml for 48 hr), transfected with CDX2, and stimulated with BMP4 (see Figure S5 for IF of CDX2). Panels are representative of three independent experiments and β-actin served as loading controls.

(B, D, and F) IF for MUC2 (upper panels, green) and K8 (lower panels, green) for the three cell lines under the same four conditions. DAPI (blue) stains the nuclei. See also Figures S5 and S6.

squamous markers *PPL*, *CRNN*, and *K13* in the EPC2-hTERT cells, and *PPL* in HET-1A cells. In both cell lines, CDX2 transfection alone did not significantly affect the expression of any of the markers including the putative CDX targets *K20* and *MUC2*. Only after stimulating the CDX2-transfected cells with BMP4, expression of *K20* and *MUC2* was significantly upregulated (Figures 4B and 4C) (McIntire et al., 2011; White et al., 2008). *K20* was recently characterized as a putative CDX1 target (Chan et al., 2009), but, under certain conditions, CDX2 can substitute CDX1 function (Savory et al., 2009). In contrast, *MUC2* has been reported as a direct target of CDX2 (Mesquita et al., 2003). *K20* and *MUC2* are highly expressed in IM and are specific markers for an intestinal phenotype.

Earlier, we and others showed that BMP4 upregulates several columnar genes (Milano et al., 2007; Wang et al., 2010). Here, we have extended our earlier findings and demonstrated that BMP4 also decreases the expression of several squamous genes at the RNA level, and, more importantly, we have found that both CDX2 and BMP4 are required to drive the expression of several specific intestinal type of genes.

BMP4 Downregulates Squamous Genes, whereas Both BMP4 and CDX2 Are Required to Induce MUC2 Protein Expression

To determine if the changes observed at the gene expression level were translated in protein expression, we analyzed primary cultures of mouse esophageal keratinocytes, HET-1A, and EPC2-hTERT cell lines by western blotting and immunofluorescence (IF). The mouse esophageal keratinocytes, EPC2-hTERT, and HET-1A cells showed efficient transfection of a CDX2-expressing vector (Figures 5A, 5C, 5E, and S5). In all cell lines, BMP4 activated the canonical BMP4/pSMAD pathway as indicated by increased expression of pSMAD. This was seen regardless of transfection with CDX2 (Figures 5A, 5C, and 5E). Activation of the BMP4/pSMAD pathway in primary keratinocytes and EPC2-hTERT cells induced downregulation of the squamous

markers p63, K5, and cytokeratin 10/13 (K10/13), whereas in HET-1A both BMP4 and CDX2 were required to downregulate K10/13 (Figures 5A, 5C, and 5E). Also independent of CDX2, BMP4/pSMAD activation showed upregulation of the columnar marker cytokeratin 8 (K8) in all three cell lines (Figures 5B, 5D, and 5F). MUC2 expression was only slightly enhanced after CDX2 transfection but increased significantly after stimulating the CDX2-transfected cells with BMP4 (Figures 5A–5F). This effect was best observed in the primary keratinocytes and EPC2-hTERT, because they have the lowest endogenous levels of pSMAD. In summary, our results confirm that BMP4 alone is able to induce the expression of columnar proteins, whereas downregulating the protein expression of several squamous genes. Furthermore, we show that activation of the BMP4/pSMAD pathway with simultaneous CDX2 expression is required to drive the expression of the intestinal specific gene MUC2.

Silencing of SMAD4 or CDX2 Decreases the Expression Level of MUC2

Because both pSMAD and CDX2 are required to induce squamous cells to express intestinal type of genes, we investigated if disruption of one of these pathways would lead to an opposite effect. First, we showed that Noggin (a natural BMP inhibitor) inhibits the canonical BMP/pSMAD pathway and induces downregulation of K8 (Figure 6A) in the BE cell line CP-A. Next, we investigated if inhibiting the translocation of the SMAD4/pSMAD complex to the nucleus would influence the expression levels of *MUC2* in CDX2 competent cells. SMAD4 is essential for translocation of pSMAD to the nucleus and for binding of the pSMAD complex to gene promoters (ten Dijke et al., 2003). The CP-A cells have a constitutively active pSMAD pathway and express *CDX2* and *MUC2*. Silencing SMAD4 using small interfering RNA (siRNA) in these cells showed a significant reduction of MUC2 expression (Figure 6B). Similarly, silencing CDX2 in CP-A cells downregulated the expression of *MUC2* (Figure 6C). These findings confirm that CDX2 regulates expression of *MUC2* (Mesquita et al., 2003; Ikeda et al., 2007; Yamamoto et al., 2003), but here we demonstrated that *MUC2* expression also depends on BMP4 downstream signaling.

pSMAD and CDX2 Form a Transcriptional Complex that Binds to the *muc2* Promoter and Is Required for *MUC2* Expression

To evaluate if pSMAD and CDX2 interact, coimmunoprecipitation (coIP) was performed on lysates of HET-1A cells transfected with CDX2 and stimulated with BMP4, and CP-A cells that endogenously express pSMAD and CDX2. Precipitation of pSMAD, using a CDX2-specific antibody (Figures 6D and 6E) was observed in both cell lysates. These findings unveil a direct interaction between pSMAD and CDX2. Sequence analysis also revealed the presence of a SMAD binding site, GTCT Smad box (Shi et al., 1998), within the CDX2 binding site of the *muc2* promoter. To investigate if the complex consisting of pSMAD and CDX2 indeed binds to the *muc2* gene promoter, chromatin immunoprecipitation (ChIP) was performed in HET-1A cells transfected with CDX2 and stimulated with BMP4. We found that the CDX2 binding region of the *muc2* promoter was enriched in the precipitated chromatin when using an antibody against pSMAD, and, as expected, when using an antibody against CDX2 (Figures 6F and 6H). Similar results were observed for human BE biopsy lysates (Figure 6H). Further evidence that CDX2 and pSMAD simultaneously engage the *muc2* promoter was obtained from the re-ChIP experiments, in which by sequentially using antibodies against pSMAD and CDX2 we again showed the pull-down of the same CDX2 binding region of the *muc2* promoter in the precipitated chromatin (Figures 6G and 6I).

In summary, we found that pSMAD and CDX2 are part of one transcriptional complex, which targets the same *muc2* gene promoter region.

CDX2 and BMP4/pSMAD activation Induce Ultrastructural Changes in Mouse Primary Keratinocytes

We studied ultrastructural changes in mouse primary keratinocytes, before and after transfection with CDX2 and/or exposure to BMP4. By transmission electron microscopy (TEM), resting untreated primary keratinocytes cells were multilayered polygonal, flattened cells (Figures 7i and ii), attached to each other via multiple attachment sites. The cells had disc-shaped, centrally placed nuclei, with perinuclear organized keratins and irregular finger-like cytoplasmic extensions surrounding them (Figures 7i and ii). These features are consistent with the normal ultrastructural appearance of squamous cells (Zboralske and Karasek, 1984). After BMP4 stimulation, the multilayered cellular organization was lost in favor of a single cell layer with flattened nuclei (Figure 7iii), and a few vacuoles within the cytoplasm (Figure 7iv). Primary keratinocytes transfected with CDX2 retained a multilayered appearance with abundant keratin (Figure 7v) and showed several cytoplasmic vacuoles and more abundant cellular extensions (Figures 7v and vi). CDX2-transfected cells exposed to BMP4 showed the formation of a single cellular layer, similar to the cells stimulated with BMP4 alone (Figures 7vii and viii). The cells contain numerous secretory vesicle-like structures. Richardson staining (Richardson et al., 1960) on epoxy semithin sections of primary mouse epithelial keratinocytes showed vacuoles that stain positive for methylene blue, a cationic dye that binds tissue anions such as ionized sulfate groups in mucins (Figure S7C). These cells also had shorter cellular extensions regularly organized at the cell surface, which resemble the formation of microvilli (Figures 7vii and viii). Noggin pretreatment of the CDX2-transfected/BMP4-treated cells prevented the BMP4 effects and retained the multi layered appearance (Figures 7ix and x). The EM results indicate that the combination of CDX2 transfection and BMP4/pSMAD pathway activation in vitro induces changes at the ultrastructural level toward a columnar-like phenotype.

DISCUSSION

The complex interplay between the BMP4/pSMAD pathway and its antagonists is essential for the development and homeostasis of the esophageal epithelium (Que et al., 2006; Rodriguez et al., 2010). It was earlier shown that the nonintestinal type of columnar esophageal metaplasia involves deregulation of this pathway but was insufficient for development of the more malignant intestinal type of BE (Wang et al., 2010; Milano et al., 2007).

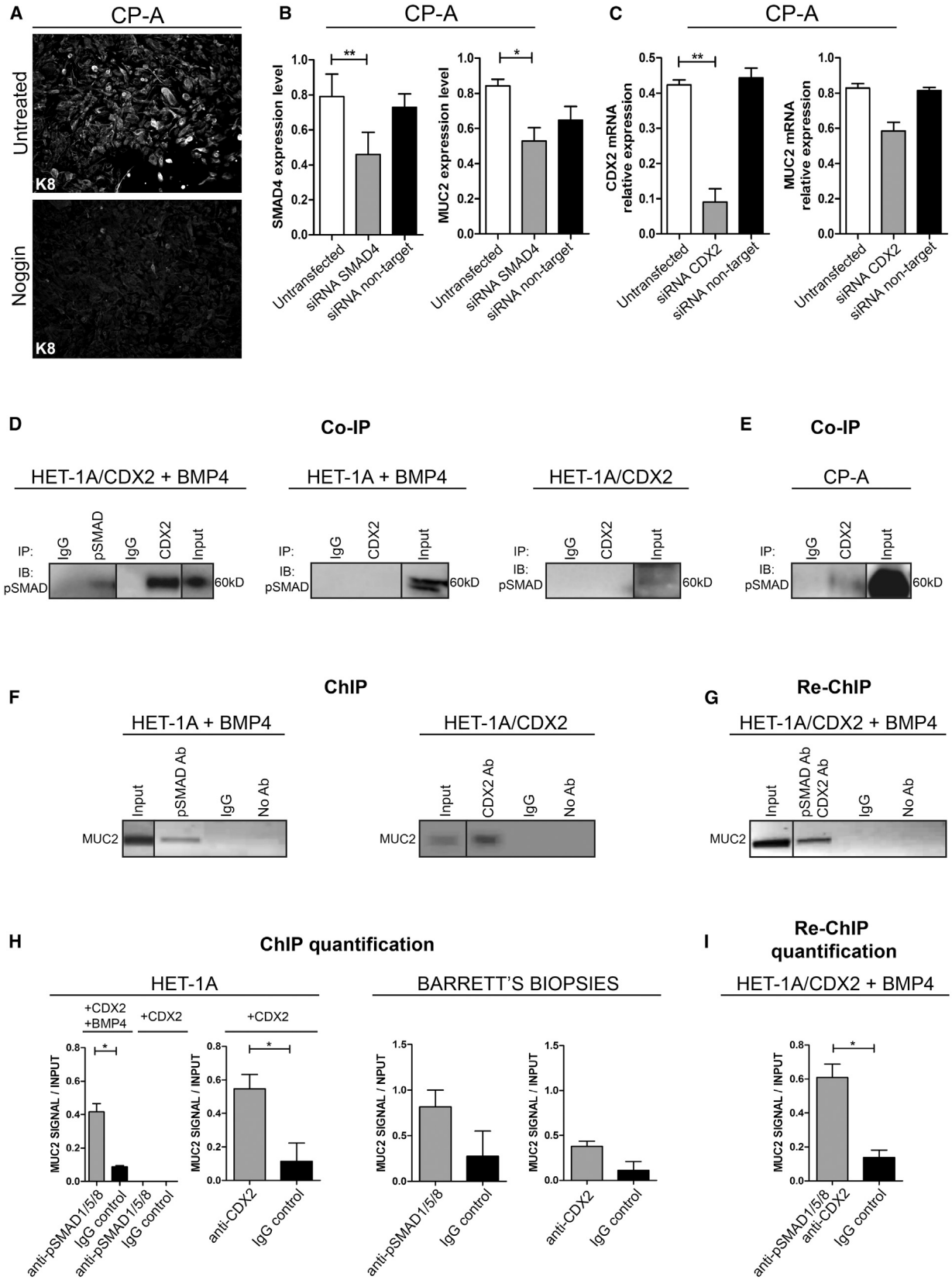

(legend on next page)

Here, we showed that BMP4-overexpressing transgenic mice developed columnar cells restricted to the SCJ. The constitutive overexpression of BMP4 in the K14-BMP4 mice seems to enhance the expression of inhibitory molecules such as Noggin compensating the BMP4 effects in proximal part of the esophagus (Figures S1A and S1B). Tissue homeostasis at junctions is complex and maintained by environmental factors, which regulate cell and tissue type (Slack, 2007). In the K14-BMP4 mice, the conflicting signals of the normal columnar stomach epithelium and the signals of the squamous epithelium favored the development of columnar metaplasia at the SCJ. Thus, at the SCJ, the environment seems to serve as a niche for (stem) cells either originating from squamous or from the columnar epithelium to give rise to metaplastic glands. The K14-BMP4 model did not account for the effects of bile reflux as observed in Barrett's patients (Quante et al., 2012; Huo et al., 2010; Kazumori et al., 2006). Bile acids have shown to induce intestinal factors such as CDX2 and MUC2 in gastric epithelial cells (Xu et al., 2010). Earlier overexpression of CDX2 in the mouse esophagus under the *k14* promoter failed to induce columnar metaplasia (Kong et al., 2011). The surgical model allowed us to identify the sequence in which various markers appear during the development of nonintestinal and intestinal metaplasia. We demonstrated that activation of the BMP4/pSMAD pathway is an early event, whereas CDX2 and MUC2 expression appear late during the development of IM. In several cell lines, we show that both factors are required to drive the expression of MUC2, which is one of the most characteristic intestinal marker. We demonstrated that these two factors form a functional complex, which binds to the *muc2* gene promoter. Based on these findings we propose that metaplastic columnar cells can differentiate further into specialized intestinal type of cells, and the pSMAD/CDX2 interaction plays a crucial role in this process. In the chromatin immunoprecipitation experiments on human BE cells, we confirmed at the molecular level that both CDX2 and pSMAD bind to the *muc2* gene promoter. Thus, in human BE, both factors are involved for the induction of MUC2 expression (Figure 6H). Besides the changes induced at the molecular level, in vitro, the plasticity of the mouse keratinocytes was also demonstrated at the ultrastructural level. We showed that the keratinocytes lost their multilayered appearance and reorganized into a monolayer, whereas the cells developed features such as microvilli when both CDX2 and pSMAD activation were induced.

Thus in vitro aberrant activation of the pSMAD/CDX2 transcriptional pathway in squamous cells leads to columnar reprogramming. However, the precise phenotypic characteristics of cells that give rise to Barrett's metaplasia in vivo still remains to be elucidated.

In humans, besides the IM recognized in the distal esophagus, metaplasia can also develop in the proximal tubular esophagus, e.g., in patients who have undergone esophagocardia resection (Castillo et al., 2012), or in the gastric cardia (Sharma et al., 2004). It is possible that each of these different organ sites involve different progenitors. In humans, the presence of the same mitochondrial mutations in squamous mucosa and BE imply a common stem cell for squamous and BE cells (Nicholson et al., 2012). The human esophageal epithelium contains complex structures such as submucosal glandular structures, which may contain different (stem) cell lineages (Glickman et al., 2001b) and is more complex than the mouse epithelium. In mice, it has been recently shown that virtually all basal cells through stochastic divisions serve as squamous progenitors (Doupé et al., 2012), whereas human squamous cells at different stages of differentiation were found to have self-renewal capacity (Barbera et al., 2014).

In an interleukin (IL)-1β-overexpressing model, it has been suggested that columnar metaplasia at the SCJ is derived from $Lgr5^+$ progenitors (Quante et al., 2012). The lineage tracing experiments in the surgical model in our study, which develops metaplasia in the mid-esophagus was, however, negative for Lgr5. Analysis of progenitor cells in different mouse models might result in conflicting outcomes, which might be dependent on the location of the metaplasia, explaining the divergent results with our $Lgr5^+$ lineage tracing experiments. Mouse models may support important observations that occur during the development of metaplasia. But these models will always fall short in deciphering the origin of the human Barrett's progenitor cell,

Figure 6. CoIP and ChIP Indicate that pSMAD and CDX2 Form a Transcriptional Complex Required for MUC2 Expression

(A) Expression of K8 by IF in the CP-A BE cell line after Noggin (100 ng/ml) treatment for 5 days (10x magnified).

(B) Quantification of SMAD4 and MUC2 levels by western blot analysis of CP-A cells lysates transfected with or without SMAD4 siRNA and nontarget siRNA. The relative expression levels of SMAD4 and MUC2 are normalized to β-actin. Representative western blot and IF panels are shown in Figure S7. Error bars indicate the SEM of the mean, paired t test *$p < 0.05$, **$p < 0.01$, $n = 3$.

(C) Quantification of *CDX2* and *MUC2* mRNA relative expression in CP-A BE cells after siRNA-mediated knockdown of CDX2. siRNA nontarget control is shown. RT-PCR data were normalized to the expression level of *GAPDH*. Error bar indicates the SEM of the mean, paired t test **$p < 0.01$, $n = 3$.

(D and E) CoIP of HET-1A cells transfected with CDX2 and stimulated with BMP4 (HET-1A/CDX2+BMP4), HET-1A only stimulated with BMP4 (HET-1A+BMP4), HET-1A only transfected with CDX2 (HET-1A/CDX2), and CP-A cells. Whole-cell lysates were immunoprecipitated (IP) with a pSMAD or a CDX2 antibody and immunoblotted (IB) with a pSMAD antibody.

(F) Representative RT-PCR image of chromatin immunoprecipitation (ChIP) experiments on nuclear extracts of HET-1A+BMP4 and HET-1A/CDX2. Input was taken as a positive control. Immunoglobulin (Ig) G and no antibody (No Ab) were taken as negative controls.

(G) Representative RT-PCR image of the Re-ChIP experiment on HET-1A/CDX2+BMP4 cells, where the chromatin is precipitated by subsequently using antibodies for pSMAD and CDX2.

(H) Quantification of the MUC2 signal from three different ChIP experiments carried out in HET-1A cells transfected with CDX2 alone (+CDX2) or transfected and treated with BMP4 (+CDX2+BMP4) and in biopsies from BE patients using pSMAD and CDX2 antibodies and IgG controls. Error bars indicate the SEM of the mean, unpaired t test *$p < 0.05$, $n = 3$.

(I) Quantification of the Re-ChiP on HET-1A/CDX2+BMP4 cells shows enrichment of the CDX2 binding region of the *muc2* gene promoter obtained by using pSMAD and CDX2 antibodies sequentially as compared to the IgG control.

Error bar indicates the SEM, unpaired t test *$p < 0.05$, $n = 3$.

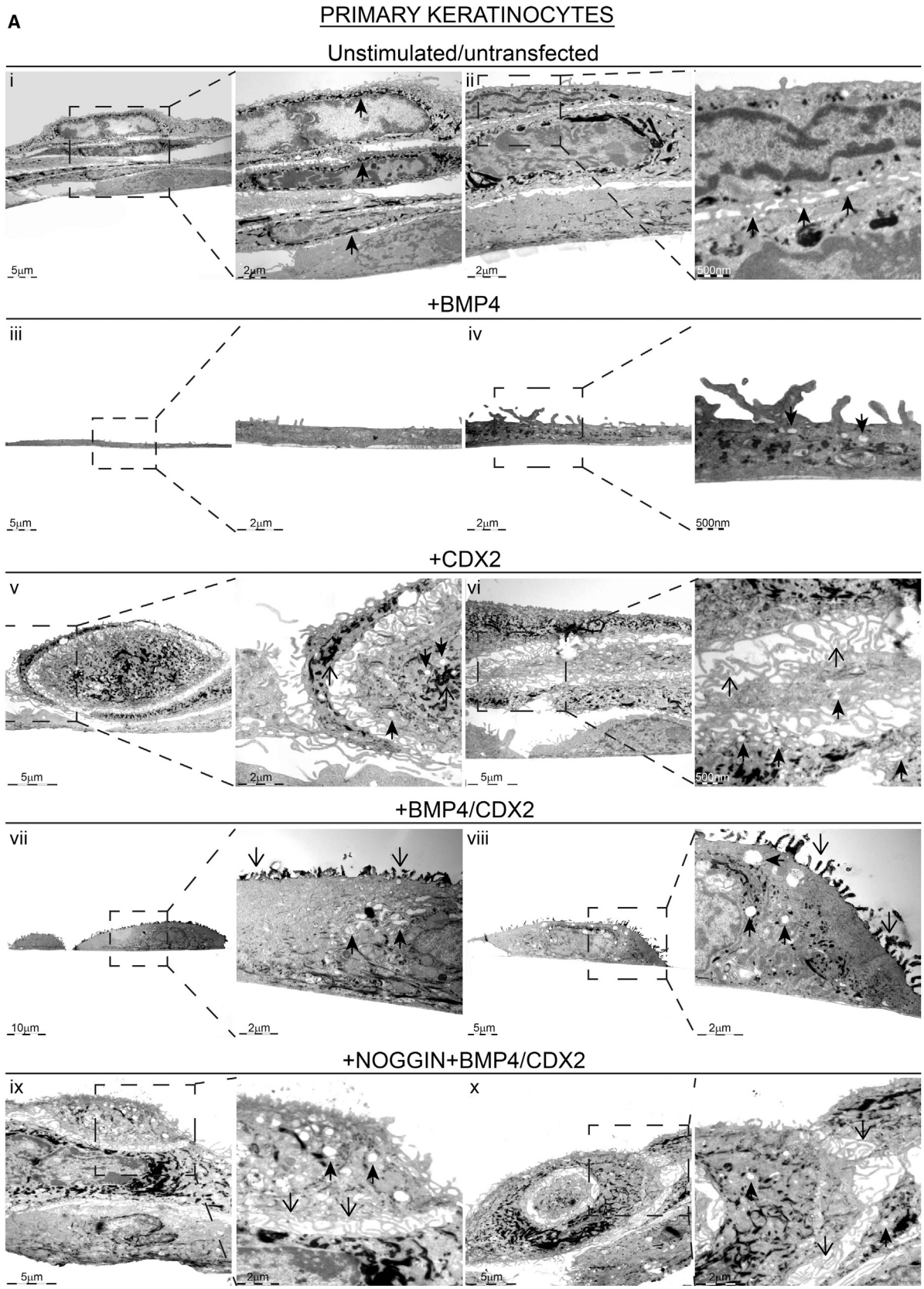

(legend on next page)

because of the fundamental anatomical differences between the human and mouse esophagus. Indeed characterizing the Barrett's progenitor cell is complex and will require analysis of human metaplastic cell populations to reveal distinct progenitor cell phenotypes. In such analyses, one will need to take into account that BE is a preneoplastic lesion acquired during adulthood. Therefore, it is possible that compared to embryonic stem cells, the Barrett's progenitor cells may present a mixed signature and for instance may also carry cancer (stem) cell features. The Barrett's preneoplastic progenitors may, for instance, resemble the more recently discovered "endogenous pluripotent somatic cell" (ePSC), identified in adult human mammary tissue, which showed to have lineage plasticity comparable to embryonic stem cells (Roy et al., 2013).

Several studies have identified other transcription factors such as SOX9, CDX1, KLF4, GATA6, HOX genes to be involved in the development of BE (Clemons et al., 2012; Kazumori et al., 2009, 2011; Wang et al., 2010; van Baal et al., 2013; di Pietro et al., 2012). We believe that this transcriptional complex may not be exclusive to pSMAD/CDX2 but may also involve several of the above-mentioned factors. Our findings provide important insight in the development of the premalignant intestinal type of differentiation. Intestinal type of metaplasia is at the basis of several malignancies (Barros et al., 2012; Spechler et al., 2010). Targeting the interaction of CDX2 and pSMAD could be an interesting strategy to reverse intestinal metaplasia in order to prevent development of the highly malignant adenocarcinoma.

EXPERIMENTAL PROCEDURES

Human Biopsy Specimens and Sampling

Informed consent and institutional ethical permission were obtained for the use of patient's biopsies. Full details about the biopsies can be found in Supplemental Experimental Procedures.

Generation of K14-BMP4 Transgenic Mice

The transgenic mice were obtained from Dr. Kessler at Northwestern University Medical School and were generated as described elsewhere (Guha et al., 2002).

Barrett's Mouse Model

Twelve CB6F1 male mice were used after formal approval of the animal ethical committee of the study. The surgical technique for inducing the esophagojejunostomy to induce reflux and metaplasia is described in Supplemental Experimental Procedures. For this study, animals were sacrificed 6, 12, and 16 weeks after the operation. Tissues of the anastomosis site were formalin fixed and paraffin embedded for IHC.

In Situ Hybridization

In situ hybridization (ISH) for *Lgr5* was carried out as described previously (Barker et al., 2007). Full details can be found in Supplemental Experimental Procedures.

Lgr5 Lineage Tracing

Lgr5-eGFP-ires-CreERT2 mice (Barker et al., 2007) were crossed with mice carrying the Rosa26LacZ reporter allele. Eight-week- old mice were injected intraperitoneally with 200 μl Tamoxifen in sunflower oil at 10 mg/ml. The surgical technique is described in Supplemental Experimental Procedures. Animals were sacrificed 6, 12, and 16 weeks after the operation. Tissues of the anastomosis site were stained for X-gal, fixed in 4% PFA overnight, and paraffin embedded.

Antibodies

All the antibodies used for the different procedures are listed in Table S1. The antimurine MUC2 antibody as characterized by Prof. J. Dekker (van Klinken et al., 1999) was kindly provided by the Erasmus University of Rotterdam.

Cell Cultures

The human SV40-T antigen immortalized esophageal epithelial cell line HET-1A was purchased from ATCC. The human hTERT immortalized esophageal cell line, EPC2-hTERT, was a kind gift of Prof. A. Rustgi, University of Pennsylvania (Harada et al., 2003). The BE cell line CP-A was provided by Dr. R. Fitzgerald (Cambridge, UK) and used with permission of Prof. P.S. Rabinovitch (Palanca-Wessels et al., 2003). Normal murine esophageal primary keratinocytes cultures were established following the protocol of J. Kalabis (Kalabis et al., 2012). Full details about the culturing methods can be found in Supplemental Experimental Procedures.

Transfection of Cells

Transfection of the cell lines was carried out as described previously (Milano et al., 2007). Full details are provided in Supplemental Experimental Procedures.

Immunohistochemistry and Immunofluorescence

Detailed IHC and IF protocols are provided in Supplemental Experimental Procedures.

RNA Isolation, RT-PCR, and Quantitative Real-Time PCR Arrays

RNA isolation was carried out as described elsewhere (Milano et al., 2007). RT-PCR was performed using the primers and conditions provided in Supplemental Experimental Procedures. Real-time qPCR was performed using customized RT^2 Profiler PCR arrays (SABiosciences) on the Roche Light Cycler 480 using RT^2 SYBR Green/qPCR Master Mix (SABiosciences). Data were normalized to the expression level of hypoxanthine phosphoribosyltransferase 1 (*HPRT1*). Full details can be found in Supplemental Experimental Procedures.

Western Blot Analysis

EPC2-hTERT and EPC2-hTERT/CDX2, HET-1A and HET-1A/CDX2, primary keratinocytes and primary keratinocytes/CDX2 cells were exposed to

Figure 7. Ultrastructural Changes in Primary Mouse Keratinocytes by Transmission Electron Microscopy

(Ai and Aii) Primary cultures of mouse keratinocytes display a multilayered organization with perinuclear keratin deposits (Ai, arrows) and multiple irregular cellular attachments (Aii, arrows).

(Aiii and Aiv) Primary keratinocytes treated with BMP4 (100 ng/ml for 5 days) show a single layered organization, a flat cellular shape and few vacuoles (Aiv, arrows).

(Av and Avi) Cells transfected with CDX2 show a multilayered organization, dense keratin deposits (Av, open arrows), cytoplasmic vacuoles (closed arrows) and elongated cellular extensions (Avi, open arrows).

(Avii and viii) After CDX2 transfection and BMP4 stimulation the cells are organized in single layer and show several secretory-like vacuoles (closed arrows) and microvilli-like structures (open arrows) on the cell surface.

(Aix and Ax) Cells treated with Noggin, before CDX2 transfection and BMP4 stimulation, retain a multilayered organization, showing similar ultrastructural changes to the cells transfected with CDX2 (Av and Avi).

See also Figure S7.

100 ng/ml BMP4 for 48 hr or left untreated. Protein lysates were processed as described earlier (Milano et al., 2007). Further details can be found in Supplemental Experimental Procedures.

RNA interference

CP-A cells were processed as previously described (Vincent et al., 2009). siRNA against SMAD4, siRNA against CDX2 and the corresponding scrambled siRNAs were used. See Supplemental Experimental Procedures for details.

Coimmunoprecipitation

Proteins were subjected to coimmunoprecipitation using a coIP kit (Pierce) and processed as previously described (Vincent et al., 2009). Details can be found in Supplemental Experimental Procedures.

Chromatin Immunoprecipitation

The ChIP assay and the Re-ChIP assay were performed as previously described (Sinkkonen et al., 2005; Bunt et al., 2010). A detailed description of the procedures is provided in Supplemental Experimental Procedures.

Transmission Electron Microscopy

Samples used for transmission electron microscopy (TEM) were processed using standard techniques. A detailed protocol can be found in Supplemental Experimental Procedures.

Statistical Analysis of Data

All experiments were repeated at least three times on independently generated samples. Representative experiments or the quantitative densitometric analysis of several experiments are shown. Data are presented as mean ± SEM and were evaluated using indicated statistical tests on Prism 5.0 software (GraphPad). A value of $p < 0.05$ was considered statistically significant.

SUPPLEMENTAL INFORMATION

Supplemental Information includes Supplemental Experimental Procedures, seven figures, and one table and can be found with this article online at http://dx.doi.org/10.1016/j.celrep.2014.03.074.

AUTHOR CONTRIBUTIONS

L.M., F.M., K.P., and D.S. performed laboratory work, acquisition of data, analysis, and interpretation of data and drafted the manuscript. V.E. and K.K.H. performed transmission electron microscopy, N.S.B. provided technical support and design of the murine model, P.F. provided funding support and drafted the manuscript, and K.K.K. provided study concept and design, drafting of the manuscript, analysis, and interpretation of data.

ACKNOWLEDGMENTS

We thank the Hubrecht laboratory of Prof. H. Clevers in Utrecht, The Netherlands for performing the RNA ISH for *Lgr5*. This work was supported by the following grants: Dutch Cancer Society and European Research Council starting grant: Targets4Barrett.

Received: February 21, 2013
Revised: December 13, 2013
Accepted: March 31, 2014
Published: May 1, 2014

REFERENCES

Barbera, M., di Pietro, M., Walker, E., Brierley, C., Macrae, S., Simons, B.D., Jones, P.H., Stingl, J., and Fitzgerald, R.C. (2014). The human squamous oesophagus has widespread capacity for clonal expansion from cells at diverse stages of differentiation. Gut, Published online February 26, 2014. http://dx.doi.org/10.1136/gutjnl-2013-306171.

Barker, N., van Es, J.H., Kuipers, J., Kujala, P., van den Born, M., Cozijnsen, M., Haegebarth, A., Korving, J., Begthel, H., Peters, P.J., and Clevers, H. (2007). Identification of stem cells in small intestine and colon by marker gene Lgr5. Nature *449*, 1003–1007.

Barros, R., Freund, J.N., David, L., and Almeida, R. (2012). Gastric intestinal metaplasia revisited: function and regulation of CDX2. Trends Mol. Med. *18*, 555–563.

Becker, L., Huang, Q., and Mashimo, H. (2010). Lgr5, an intestinal stem cell marker, is abnormally expressed in Barrett's esophagus and esophageal adenocarcinoma. Dis. Esophagus *23*, 168–174.

Bunt, J., de Haas, T.G., Hasselt, N.E., Zwijnenburg, D.A., Koster, J., Versteeg, R., and Kool, M. (2010). Regulation of cell cycle genes and induction of senescence by overexpression of OTX2 in medulloblastoma cell lines. Mol. Cancer Res. *8*, 1344–1357.

Castillo, D., Puig, S., Iglesias, M., Seoane, A., de Bolós, C., Munitiz, V., Parrilla, P., Comerma, L., Poulsom, R., Krishnadath, K.K., et al. (2012). Activation of the BMP4 pathway and early expression of CDX2 characterize non-specialized columnar metaplasia in a human model of Barrett's esophagus. J. Gastrointest. Surg. *16*, 227–237, discussion 237.

Chan, C.W., Wong, N.A., Liu, Y., Bicknell, D., Turley, H., Hollins, L., Miller, C.J., Wilding, J.L., and Bodmer, W.F. (2009). Gastrointestinal differentiation marker Cytokeratin 20 is regulated by homeobox gene CDX1. Proc. Natl. Acad. Sci. USA *106*, 1936–1941.

Chandrasoma, P. (1997). Pathophysiology of Barrett's esophagus. Semin. Thorac. Cardiovasc. Surg. *9*, 270–278.

Chandrasoma, P., Wickramasinghe, K., Ma, Y., and DeMeester, T. (2007). Is intestinal metaplasia a necessary precursor lesion for adenocarcinomas of the distal esophagus, gastroesophageal junction and gastric cardia? Dis. Esophagus *20*, 36–41.

Chaves, P., Pereira, A.D., Cruz, C., Suspiro, A., Mendes de Almeida, J.C., Leitão, C.N., and Soares, J. (2002). Recurrent columnar-lined esophageal segments—study of the phenotypic characteristics using intestinal markers. Dis. Esophagus *15*, 282–286.

Chen, X., Qin, R., Liu, B., Ma, Y., Su, Y., Yang, C.S., Glickman, J.N., Odze, R.D., and Shaheen, N.J. (2008). Multilayered epithelium in a rat model and human Barrett's esophagus: similar expression patterns of transcription factors and differentiation markers. BMC Gastroenterol. *8*, 1.

Clemons, N.J., Wang, D.H., Croagh, D., Tikoo, A., Fennell, C.M., Murone, C., Scott, A.M., Watkins, D.N., and Phillips, W.A. (2012). Sox9 drives columnar differentiation of esophageal squamous epithelium: a possible role in the pathogenesis of Barrett's esophagus. Am. J. Physiol. Gastrointest. Liver Physiol. *303*, G1335–G1346.

di Pietro, M., Lao-Sirieix, P., Boyle, S., Cassidy, A., Castillo, D., Saadi, A., Eskeland, R., and Fitzgerald, R.C. (2012). Evidence for a functional role of epigenetically regulated midcluster HOXB genes in the development of Barrett esophagus. Proc. Natl. Acad. Sci. USA *109*, 9077–9082.

Doupé, D.P., Alcolea, M.P., Roshan, A., Zhang, G., Klein, A.M., Simons, B.D., and Jones, P.H. (2012). A single progenitor population switches behavior to maintain and repair esophageal epithelium. Science *337*, 1091–1093.

Glickman, J.N., Chen, Y.Y., Wang, H.H., Antonioli, D.A., and Odze, R.D. (2001a). Phenotypic characteristics of a distinctive multilayered epithelium suggests that it is a precursor in the development of Barrett's esophagus. Am. J. Surg. Pathol. *25*, 569–578.

Glickman, J.N., Yang, A., Shahsafaei, A., McKeon, F., and Odze, R.D. (2001b). Expression of p53-related protein p63 in the gastrointestinal tract and in esophageal metaplastic and neoplastic disorders. Hum. Pathol. *32*, 1157–1165.

Griffiths, E.A., Pritchard, S.A., McGrath, S.M., Valentine, H.R., Price, P.M., Welch, I.M., and West, C.M. (2007). Increasing expression of hypoxia-inducible proteins in the Barrett's metaplasia-dysplasia-adenocarcinoma sequence. Br. J. Cancer *96*, 1377–1383.

Guha, U., Gomes, W.A., Kobayashi, T., Pestell, R.G., and Kessler, J.A. (2002). In vivo evidence that BMP signaling is necessary for apoptosis in the mouse limb. Dev. Biol. *249*, 108–120.

Harada, H., Nakagawa, H., Oyama, K., Takaoka, M., Andl, C.D., Jacobmeier, B., von Werder, A., Enders, G.H., Opitz, O.G., and Rustgi, A.K. (2003). Telomerase induces immortalization of human esophageal keratinocytes without p16INK4a inactivation. Mol. Cancer Res. *1*, 729–738.

Huo, X., Zhang, H.Y., Zhang, X.I., Lynch, J.P., Strauch, E.D., Wang, J.Y., Melton, S.D., Genta, R.M., Wang, D.H., Spechler, S.J., and Souza, R.F. (2010). Acid and bile salt-induced CDX2 expression differs in esophageal squamous cells from patients with and without Barrett's esophagus. Gastroenterology *139*, 194–203, e1.

Ikeda, H., Sasaki, M., Ishikawa, A., Sato, Y., Harada, K., Zen, Y., Kazumori, H., and Nakanuma, Y. (2007). Interaction of Toll-like receptors with bacterial components induces expression of CDX2 and MUC2 in rat biliary epithelium in vivo and in culture. Lab. Invest. *87*, 559–571.

Kalabis, J., Wong, G.S., Vega, M.E., Natsuizaka, M., Robertson, E.S., Herlyn, M., Nakagawa, H., and Rustgi, A.K. (2012). Isolation and characterization of mouse and human esophageal epithelial cells in 3D organotypic culture. Nat. Protoc. *7*, 235–246.

Kazumori, H., Ishihara, S., Rumi, M.A., Kadowaki, Y., and Kinoshita, Y. (2006). Bile acids directly augment caudal related homeobox gene Cdx2 expression in oesophageal keratinocytes in Barrett's epithelium. Gut *55*, 16–25.

Kazumori, H., Ishihara, S., and Kinoshita, Y. (2009). Roles of caudal-related homeobox gene Cdx1 in oesophageal epithelial cells in Barrett's epithelium development. Gut *58*, 620–628.

Kazumori, H., Ishihara, S., Takahashi, Y., Amano, Y., and Kinoshita, Y. (2011). Roles of Kruppel-like factor 4 in oesophageal epithelial cells in Barrett's epithelium development. Gut *60*, 608–617.

Kong, J., Crissey, M.A., Funakoshi, S., Kreindler, J.L., and Lynch, J.P. (2011). Ectopic Cdx2 expression in murine esophagus models an intermediate stage in the emergence of Barrett's esophagus. PLoS ONE *6*, e18280.

Liu, T., Zhang, X., So, C.K., Wang, S., Wang, P., Yan, L., Myers, R., Chen, Z., Patterson, A.P., Yang, C.S., and Chen, X. (2007). Regulation of Cdx2 expression by promoter methylation, and effects of Cdx2 transfection on morphology and gene expression of human esophageal epithelial cells. Carcinogenesis *28*, 488–496.

McIntire, M.G., Soucy, G., Vaughan, T.L., Shahsafaei, A., and Odze, R.D. (2011). MUC2 is a highly specific marker of goblet cell metaplasia in the distal esophagus and gastroesophageal junction. Am. J. Surg. Pathol. *35*, 1007–1013.

Means, A.L., Xu, Y., Zhao, A., Ray, K.C., and Gu, G. (2008). A CK19(CreERT) knockin mouse line allows for conditional DNA recombination in epithelial cells in multiple endodermal organs. Genesis *46*, 318–323.

Mesquita, P., Jonckheere, N., Almeida, R., Ducourouble, M.P., Serpa, J., Silva, E., Pigny, P., Silva, F.S., Reis, C., Silberg, D., et al. (2003). Human MUC2 mucin gene is transcriptionally regulated by Cdx homeodomain proteins in gastrointestinal carcinoma cell lines. J. Biol. Chem. *278*, 51549–51556.

Milano, F., van Baal, J.W., Buttar, N.S., Rygiel, A.M., de Kort, F., DeMars, C.J., Rosmolen, W.D., Bergman, J.J., VAn Marle, J., Wang, K.K., et al. (2007). Bone morphogenetic protein 4 expressed in esophagitis induces a columnar phenotype in esophageal squamous cells. Gastroenterology *132*, 2412–2421.

Mutoh, H., Hakamata, Y., Sato, K., Eda, A., Yanaka, I., Honda, S., Osawa, H., Kaneko, Y., and Sugano, K. (2002). Conversion of gastric mucosa to intestinal metaplasia in Cdx2-expressing transgenic mice. Biochem. Biophys. Res. Commun. *294*, 470–479.

Nemeth, I.B., Rosztoczy, A., Izbeki, F., Roka, R., Gecse, K., Sukosd, F., Nyari, T., Wittmann, T., and Tiszlavicz, L. (2012). A renewed insight into Barrett's esophagus: comparative histopathological analysis of esophageal columnar metaplasia. Dis. Esophagus *25*, 395–402.

Nicholson, A.M., Graham, T.A., Simpson, A., Humphries, A., Burch, N., Rodriguez-Justo, M., Novelli, M., Harrison, R., Wright, N.A., McDonald, S.A., and Jankowski, J.A. (2012). Barrett's metaplasia glands are clonal, contain multiple stem cells and share a common squamous progenitor. Gut *61*, 1380–1389.

Palanca-Wessels, M.C., Klingelhutz, A., Reid, B.J., Norwood, T.H., Opheim, K.E., Paulson, T.G., Feng, Z., and Rabinovitch, P.S. (2003). Extended lifespan of Barrett's esophagus epithelium transduced with the human telomerase catalytic subunit: a useful in vitro model. Carcinogenesis *24*, 1183–1190.

Quante, M., Marrache, F., Goldenring, J.R., and Wang, T.C. (2010). TFF2 mRNA transcript expression marks a gland progenitor cell of the gastric oxyntic mucosa. Gastroenterology *139*, 2018–2027, e2.

Quante, M., Bhagat, G., Abrams, J.A., Marache, F., Good, P., Lee, M.D., Lee, Y., Friedman, R., Asfaha, S., Dubeykovskaya, Z., et al. (2012). Bile acid and inflammation activate gastric cardia stem cells in a mouse model of Barrett-like metaplasia. Cancer Cell *21*, 36–51.

Que, J., Choi, M., Ziel, J.W., Klingensmith, J., and Hogan, B.L. (2006). Morphogenesis of the trachea and esophagus: current players and new roles for noggin and Bmps. Differentiation *74*, 422–437.

Richardson, K.C., Jarett, L., and Finke, E.H. (1960). Embedding in epoxy resins for ultrathin sectioning in electron microscopy. Stain Technol. *35*, 313–323.

Rodriguez, P., Da Silva, S., Oxburgh, L., Wang, F., Hogan, B.L., and Que, J. (2010). BMP signaling in the development of the mouse esophagus and forestomach. Development *137*, 4171–4176.

Roy, S., Gascard, P., Dumont, N., Zhao, J., Pan, D., Petrie, S., Margeta, M., and Tlsty, T.D. (2013). Rare somatic cells from human breast tissue exhibit extensive lineage plasticity. Proc. Natl. Acad. Sci. USA *110*, 4598–4603.

Savory, J.G., Pilon, N., Grainger, S., Sylvestre, J.R., Béland, M., Houle, M., Oh, K., and Lohnes, D. (2009). Cdx1 and Cdx2 are functionally equivalent in vertebral patterning. Dev. Biol. *330*, 114–122.

Senoo, M., Pinto, F., Crum, C.P., and McKeon, F. (2007). p63 Is essential for the proliferative potential of stem cells in stratified epithelia. Cell *129*, 523–536.

Sharma, P., McElhinney, C., Topalovski, M., Mayo, M.S., McGregor, D.H., and Weston, A. (2004). Detection of cardia intestinal metaplasia: do the biopsy number and location matter? Am. J. Gastroenterol. *99*, 2424–2428.

Shi, Y., Wang, Y.F., Jayaraman, L., Yang, H., Massagué, J., and Pavletich, N.P. (1998). Crystal structure of a Smad MH1 domain bound to DNA: insights on DNA binding in TGF-beta signaling. Cell *94*, 585–594.

Sinkkonen, L., Malinen, M., Saavalainen, K., Väisänen, S., and Carlberg, C. (2005). Regulation of the human cyclin C gene via multiple vitamin D3-responsive regions in its promoter. Nucleic Acids Res. *33*, 2440–2451.

Slack, J.M. (2007). Metaplasia and transdifferentiation: from pure biology to the clinic. Nat. Rev. Mol. Cell Biol. *8*, 369–378.

Spechler, S.J., Fitzgerald, R.C., Prasad, G.A., and Wang, K.K. (2010). History, molecular mechanisms, and endoscopic treatment of Barrett's esophagus. Gastroenterology *138*, 854–869.

Srivastava, A., Odze, R.D., Lauwers, G.Y., Redston, M., Antonioli, D.A., and Glickman, J.N. (2007). Morphologic features are useful in distinguishing Barrett esophagus from carditis with intestinal metaplasia. Am. J. Surg. Pathol. *31*, 1733–1741.

Steininger, H., Pfofe, D.A., Müller, H., Haag-Sunjic, G., and Fratianu, V. (2005). Expression of CDX2 and MUC2 in Barrett's mucosa. Pathol. Res. Pract. *201*, 573–577.

ten Dijke, P., Korchynskyi, O., Valdimarsdottir, G., and Goumans, M.J. (2003). Controlling cell fate by bone morphogenetic protein receptors. Mol. Cell. Endocrinol. *211*, 105–113.

Underwood, T.J., Derouet, M.F., White, M.J., Noble, F., Moutasim, K.A., Smith, E., Drew, P.A., Thomas, G.J., Primrose, J.N., and Blaydes, J.P. (2010). A comparison of primary oesophageal squamous epithelial cells with HET-1A in organotypic culture. Biol. Cell *102*, 635–644.

van Baal, J.W., Verbeek, R.E., Bus, P., Fassan, M., Souza, R.F., Rugge, M., ten Kate, F.J., Vleggaar, F.P., and Siersema, P.D. (2013). microRNA-145 in Barrett's oesophagus: regulating BMP4 signalling via GATA6. Gut *62*, 664–675.

van Klinken, B.J., Einerhand, A.W., Duits, L.A., Makkink, M.K., Tytgat, K.M., Renes, I.B., Verburg, M., Büller, H.A., and Dekker, J. (1999). Gastrointestinal expression and partial cDNA cloning of murine Muc2. Am. J. Physiol. *276*, G115–G124.

Vincent, T., Neve, E.P., Johnson, J.R., Kukalev, A., Rojo, F., Albanell, J., Pietras, K., Virtanen, I., Philipson, L., Leopold, P.L., et al. (2009). A SNAIL1-SMAD3/4 transcriptional repressor complex promotes TGF-beta mediated epithelial-mesenchymal transition. Nat. Cell Biol. *11*, 943–950.

von Rahden, B.H., Kircher, S., Lazariotou, M., Reiber, C., Stuermer, L., Otto, C., Germer, C.T., and Grimm, M. (2011). LgR5 expression and cancer stem cell hypothesis: clue to define the true origin of esophageal adenocarcinomas with and without Barrett's esophagus? J. Exp. Clin. Cancer Res. *30*, 23.

Wang, J., Qin, R., Ma, Y., Wu, H., Peters, H., Tyska, M., Shaheen, N.J., and Chen, X. (2009). Differential gene expression in normal esophagus and Barrett's esophagus. J. Gastroenterol. *44*, 897–911.

Wang, D.H., Clemons, N.J., Miyashita, T., Dupuy, A.J., Zhang, W., Szczepny, A., Corcoran-Schwartz, I.M., Wilburn, D.L., Montgomery, E.A., Wang, J.S., et al. (2010). Aberrant epithelial-mesenchymal Hedgehog signaling characterizes Barrett's metaplasia. Gastroenterology *138*, 1810–1822.

White, N.M., Gabril, M., Ejeckam, G., Mathews, M., Fardy, J., Kamel, F., Doré, J., and Yousef, G.M. (2008). Barrett's esophagus and cardiac intestinal metaplasia: two conditions within the same spectrum. Can. J. Gastroenterol. *22*, 369–375.

Xu, Y., Watanabe, T., Tanigawa, T., Machida, H., Okazaki, H., Yamagami, H., Watanabe, K., Tominaga, K., Fujiwara, Y., Oshitani, N., and Arakawa, T. (2010). Bile acids induce cdx2 expression through the farnesoid x receptor in gastric epithelial cells. J. Clin. Biochem. Nutr. *46*, 81–86.

Yamamoto, H., Bai, Y.Q., and Yuasa, Y. (2003). Homeodomain protein CDX2 regulates goblet-specific MUC2 gene expression. Biochem. Biophys. Res. Commun. *300*, 813–818.

Yang, A., Schweitzer, R., Sun, D., Kaghad, M., Walker, N., Bronson, R.T., Tabin, C., Sharpe, A., Caput, D., Crum, C., and McKeon, F. (1999). p63 is essential for regenerative proliferation in limb, craniofacial and epithelial development. Nature *398*, 714–718.

Zboralske, F.F., and Karasek, M.A. (1984). Growth characteristics of human esophageal epithelial cells in primary explant and serial culture. In Vitro *20*, 109–118.